Synthesis, Crystal Structure, UV-vis and EPR Studies of $(NH_3CH_2CH_2NH_2)_{2.5}[Mo^{(V)}_{0.5}W^{(VI)}_{0.5}O_2(OC_6H_4O)_2]$

LU, Xiao-Ming*,[a,b] (鲁晓明) SONG, Fu-Gen[a] (宋富根) LOU, Fu-Yan[a] (娄福艳)
MAO, Xi-An[b] (毛希安) YE, Zhao-Hui[b] (叶朝辉) LU, Jing-Fen[c] (卢景芬)
[a] *Department of Chemistry, Capital Normal University, Beijing 100037, China*
[b] *Wuhan Institute of Physics and Mathematics, Chinese Academy of Sciences, Wuhan, Hubei 430071, China*
[c] *State Key Laboratory of Natural and Biomimetic Drugs, Medicine Science Center, Peking University, Beijing 100083, China*

***Cis*-dioxo-metal complex $(NH_3CH_2CH_2NH_2)_{2.5}[Mo^{(V)}_{0.5}W^{(VI)}_{0.5}O_2(OC_6H_4O)_2]$ 1 was obtained by the reaction of tetra-butyl ammonium hexamolybdotungstate with 1,2-dihydroxybenzene in the mixed solvent of CH_3OH, CH_3CN and ethylenediamine, and characterized by X-ray diffraction, UV-vis and EPR analysis. Compared with its analogous complexes $(NH_3CH_2CH_2NH_2)_3[Mo^{(V)}O_2(OC_6H_4O)_2]$ 2 and $(NH_3CH_2CH_2NH_2)_2[W^{(VI)}O_2(OC_6H_4O)_2]$ 3, the results show that tungsten(VI) is less active in redox than molybdenum(VI) and that the change of the valence induced by substitution of W(VI) for Mo(V) in $[MO_2(OC_6H_4O)_2]^{n-}$ does not influence the coordination geometry of the complex anion in which the metal center exhibits distorted octahedral coordination with *cis*-dioxo catechol. The responses to EPR of complexes 1 and 2 are active but complex 3 is silent, and the UV-vis spectra exhibited by the three complexes are obvious different because of the different electronic configuration between the central Mo(V) and W(VI) ions in the complexes. It is noteworthy that complexes 1 and 2 have the similar EPR signal to flavoenzyme, suggesting that the three complexes have the same coordination geometry feature with the co-factor of flavoenzyme.**

Keywords *cis*-dioxo-molybdo(V)tungsten(VI) complex, 1,2-dihydroxybenzene, EPR, UV-vis, octahedral coordination

Introduction

Variable-valence molybdenum complexes with oxo and sulfido ligation have attracted considerable attention for a long time, because they are related to the class of oxotransfer enzymes such as xanthine oxidase, sulfite oxidase and nitrate reductase, which transfer oxygen atom to and from biological substrates in the nitrogen, sulfur and carbon cycles.[1] Since the first naturally occurring tungstenenzyme was purified in 1983 tungsten complexes with oxo and sulfido have made a dramatic progress particularly in recent years.[2] Especially the *cis*-MoO_2 and *cis*-WO_2 units are more important in molybdenum and tungsten chemistry, because they occur at the active site in some molybdenum and tungsten oxotransferase enzymes and play role as "spectator" in the primary oxygen atom transfer process.[3-8] Moreover, as the known Mo(V) and W(V) compounds are EPR active due to their d^1 electronic configuration, EPR spectroscopy has become one of the most powerful technique for study of Mo and W chemistry, and help us to understand the coordination structure of Mo and W and the electron transfer process in molybdenum and tungsten enzymes. Notably, for almost the known tungstoenzymes there is an analogous molybdoenzyme within the same organism or in a very closely related species.[2] However studying the structure of the active site in molybdenum and tungsten oxotransferase enzymes is difficult due to the complexity and delicate nature of the proteins, and the preparation of the enzyme for X-ray crystal structure analysis may result in changes in the active site. Moreover Mo(V) and W(V) intermediates are hardly obtained and Mo(V) and W(V) complexes are rarely reported because of their activity in redox process. Herein we describe the synthesis and the crystal structure of $(NH_3CH_2CH_2NH_2)_{2.5}[Mo^{(V)}_{0.5}W^{(VI)}_{0.5}O_2(OC_6H_4O)_2]$, and make a comparison of the UV-vis spectra exhibited by the title complex and its analogous complexes $(NH_3CH_2CH_2NH_2)_3[Mo^{(VI)}O_2(OC_6H_4O)_2]$ and $(NH_3CH_2CH_2NH_2)_2[W^{(VI)}O_2(OC_6H_4O)_2]$. We also study the EPR spectra of the three complexes and flavoenzyme from milk.

Experimental

Materials and methods

All reagents used were received from commercial supplies. All manipulations were carried out in the laboratory atmosphere. Elemental C, H, N analysis and W, Mo

* E-mail: lu-xiaoming@263.net
Received November 15, 2002; revised March 3, 2003; accepted July 10, 2003.
Project supported by the National Natural Science Foundation of China (No. 20271034), the Natural Science Foundation of Beijing (No. 2012005) and the Natural Science Foundation of Educational Ministry of Beijing.

analysis were performed on a Perkin-Elmer analyzer and an ICP-AAS(ICP-8410) analyzer respectively. Infrared spectra were recorded as KBr pellets on a Perkin-Elmer 1600 Series FT IR spectrometer. UV-vis spectra were recorded in 10 mm quartz cell on a shimadzu UV-265 instrument. EPR spectra were measured with Bruke-300 EPR spectrometer.

Synthesis

$(NH_3CH_2CH_2NH_2)_{2.5}[Mo^{(V)}_{0.5}W^{(VI)}_{0.5}O_2(OC_6H_4O)_2]$

An addition of $(n\text{-}Bu)_4NBr$ to a solution of $Na_2MoO_4\cdot 2H_2O$ (12.5 g) and $Na_2WO_4\cdot 2H_2O$ (6.5 g) adjusted to pH = 3.5 with chloric acid (30%) resulted in yellow powder. The yellow powder (1.50 g) and 1,2-dihydroxybenzene (0.80 g) were put in the mixed solvent of CH_3OH (25 mL), CH_3CN (25 mL) and $NH_2CH_2CH_2NH_2$ (5 mL), stirred for 6 h and filtered. The filtrate was layered with Et_2O for a week and red crystal $(NH_3CH_2CH_2NH_2)_{2.5}[Mo^{(V)}_{0.5}W^{(VI)}_{0.5}O_2(OC_6H_4O)_2]$ was obtained and air-stable. Anal. calcd for $C_{17}H_{30}Mo_{0.5}N_5O_6W_{0.5}$: C 7.79, H 5.61, N 12.96, Mo 8.88, W 17.01; found C 37.57, H 5.57, N 12.89, Mo 8.94, W 17.02.

Crystallography

Single-crystal X-ray diffraction measurements were carried out with a Brucker Smart 1000 CCD at (293 ± 2) K. The diffractometer was equipped with a graphite crystal monochromator situated in the incident beam for data collection. The determination of unit cell parameters and data collections were performed with Mo Kα radiation (λ = 0.071073 nm). Unit cell dimensions were obtained with least-squares refinements, and all the structures were solved by direct methods. Mo and W atoms in the complex were located from E-map. The other non-hydrogen atoms were located in successive difference Fourier syntheses. The final refinement was performed by full-matrix least-squires method with anisotropic thermal parameters for non-hydrogen atoms on F^2. The hydrogen atoms were added theoretically, riding on the concerned atoms and refined with fixed thermal factors. Crystallographic data and experimental details for structural analysis of complex **(1)** are summarized in Table 1 and the bond lengths and angles are listed in Table 2.

Table 1 Crystal data for $(NH_2CH_2CH_2NH_3)_{2.5}[Mo^{(V)}_{0.5}W^{(VI)}_{0.5}O_2(OC_6H_4O)_2]$

Formula	$C_{17}H_{30}Mo_{0.50}N_5O_6W_{0.50}$
M_r	540.35
T (K)	293(2)
Space group	$P2(1)/c$
a (nm)	0.71276(5)
b (nm)	3.0778(2)
c (nm)	0.98087(7)
β (°)	102.6040(10)
V (nm^3)	5.038(3)
Z	4
ρ_{calcd} (g·cm^{-3})	1.709
μ (cm^{-1})	31.06
R	0.0288
R_w	0.0781

Table 2 Bond lengths ($\times 10^{-1}$ nm) and angles (°) for complex **1**[a]

M(1)—O(1)	1.733(4)	M(1)—O(2)	1.745(4)	M(1)—O(4)	1.974(3)
M(1)—O(5)	1.991(4)	M(1)—O(3)	2.132(4)	M(1)—O(6)	2.146(3)
O(3)—C(1)	1.333(6)	O(4)—C(2)	1.361(6)	O(5)—C(7)	1.359(7)
O(6)—C(8)	1.348(6)	C(1)—C(6)	1.394(7)	C(1)—C(2)	1.401(8)
C(2)—C(3)	1.395(8)	C(3)—C(4)	1.400(10)	C(4)—C(5)	1.376(11)
C(5)—C(6)	1.399(10)	C(7)—C(12)	1.385(7)	C(7)—C(8)	1.399(7)
C(8)—C(9)	1.384(7)	C(9)—C(10)	1.394(8)	C(10)—C(11)	1.372(9)
C(11)—C(12)	1.379(9)	C(13)—N(1)	1.484(6)	C(13)—C(14)	1.508(7)
C(14)—N(2)	1.453(7)	C(15)—N(3)	1.468(7)	C(15)—C(16)	1.518(8)
C(16)—N(4)	1.442(7)	C(17)—N(5)	1.459(7)	C(17)—C(17) #1	1.494(11)
O(1)-M(1)-O(2)	102.82(18)	O(1)-M(1)-O(4)	89.94(17)	O(2)-M(1)-O(4)	102.28(17)
O(1)-M(1)-O(5)	103.79(18)	O(2)-M(1)-O(5)	89.45(17)	O(4)-M(1)-O(5)	159.62(15)
O(1)-M(1)-O(3)	161.84(17)	O(2)-M(1)-O(3)	91.84(17)	O(4)-M(1)-O(3)	76.35(15)
O(5)-M(1)-O(3)	86.79(14)	O(1)-M(1)-O(6)	87.75(16)	O(2)-M(1)-O(6)	163.94(16)
O(4)-M(1)-O(6)	89.64(14)	O(5)-M(1)-O(6)	76.16(14)	O(3)-M(1)-O(6)	80.42(15)
C(1)-O(3)-M(1)	113.9(3)	C(2)-O(4)-M(1)	118.6(3)	C(7)-O(5)-M(1)	118.8(3)
C(8)-O(6)-M(1)	114.4(3)	O(3)-C(1)-C(6)	125.6(5)	O(3)-C(1)-C(2)	115.3(4)
C(6)-C(1)-C(2)	119.0(5)	O(4)-C(2)-C(3)	123.0(5)	O(4)-C(2)-C(1)	114.8(4)
C(3)-C(2)-C(1)	122.2(5)	C(2)-C(3)-C(4)	117.3(6)	C(5)-C(4)-C(3)	121.5(6)
C(4)-C(5)-C(6)	120.6(6)	C(1)-C(6)-C(5)	119.3(7)	O(5)-C(7)-C(12)	123.9(5)

Continued

O(5)-C(7)-C(8)	115.8(4)	C(12)-C(7)-C(8)	120.3(5)	O(6)-C(8)-C(9)	125.2(5)
O(6)-C(8)-C(7)	114.7(5)	C(9)-C(8)-C(7)	120.1(5)	C(10)-C(9)-C(8)	118.7(5)
C(11)-C(10)-C(9)	121.1(6)	C(10)-C(11)-C(12)	120.4(5)	C(11)-C(12)-C(7)	119.4(5)
N(1)-C(13)-C(14)	112.6(4)	N(2)-C(14)-C(13)	112.4(4)	N(3)-C(15)-C(16)	112.0(5)
N(4)-C(16)-C(15)	115.6(5)	N(5)-C(17)-C(17) # 1	111.8(6)		

[a] M = Mo and W; symmetry transformations used to generate equivalent atoms: # 1 $-x+2$, $-y+1$, $-z+1$.

Results and discussion

Description of crystal structure

The complex anion structure of $[Mo^{(V)}_{0.5}W^{(VI)}_{0.5}O_2(OC_6H_4O)_2]^{2.5-}$ is shown in Fig. 1. The structure of the mononuclear anionic unit displays the *cis*-dioxo fashion with pseudo-octahedral $[MO_6]$ coordination geometry in which the central metal position is occupied by a half of Mo(V) and a half of W(VI). The terminal metal-oxo distances are within the range of 0.1733(4)—0.1745(4) nm which are close to pure tungsten-oxo distances [0.1741(5)—0.1744(5) nm] and a little longer than pure molybdenum-oxo distances [0.1702(6)—0.1709(5) nm] as presented in Table 3. The trans influence of the oxo groups is evident in the nonequivalent M—O (ligand) distances, averaging 0.1983(4) and 0.2139(4) nm for ligation *cis* and *trans* to the oxo groups in $[Mo^{(V)}_{0.5}W^{(VI)}_{0.5}O_2(OC_6H_4O)_2]^{2.5-}$. The 2 + 2 + 2 pattern of M—O distances is exhibited in the bonding parameters by the complex anions. The structures of $[Mo^{(V)}O_2(OC_6H_4O)_2]^{3-}$[9] and $[W^{(VI)}O_2(OC_6H_4O)_2]^{2-}$[10] are similar to $[Mo^{(V)}_{0.5}W^{(VI)}_{0.5}O_2(OC_6H_4O)_2]^{2.5-}$, and there are no much differences among the complexes in coordination geometry except a little change in bond length as presented in Table 3.

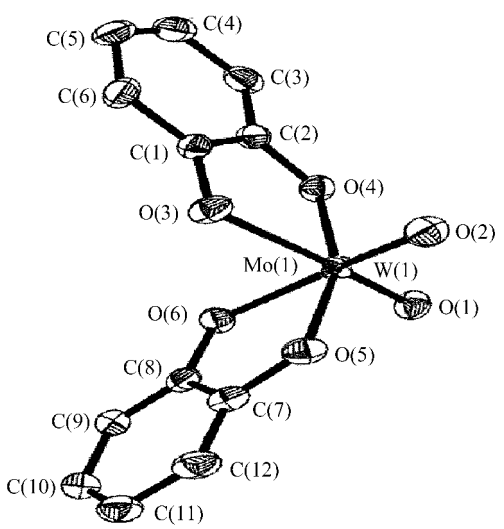

Fig. 1 Structure of $[Mo^{(V)}_{0.5}W^{(VI)}_{0.5}O_2(OC_6H_4O)_2]^{2.5-}$.

It is worthy to note that the central $Mo^{(V)}$ and $W^{(VI)}$ ions have different electronic configuration in $[Mo^{(V)}_{0.5}W^{(VI)}_{0.5}O_2(OC_6H_4O)_2]^{2.5-}$, $[Mo^{(V)}O_2(OC_6H_4O)_2]^{3-}$ and $[W^{(VI)}O_2(OC_6H_4O)_2]^{2-}$. The result implies that tungsten (VI) is less active in redox than molybdenum (VI) and the change of the valence induced by substitution of W(VI) for Mo(V) in $[MO_2(OC_6H_4O)_2]^{n-}$ does not influence the coordination geometry of the complex anions. Two and half mono-protonated ethylenediamine anti-counter cations are needed to satisfy the charge requirement of $[Mo^{(V)}_{0.5}W^{(VI)}_{0.5}O_2(OC_6H_4O)_2]^{2.5-}$.

Table 3 The selected bond lengths of complexex **1**, **2** and **3**[a]

	Complex **2**	Complex **1**	Complex **3**
M—O_t	1.702(6)	1.733(4)	1.741(5)
	1.709(5)	1.745(4)	1.744(5)
M—O(Ar)	2.007(6)	1.974(3)	1.9819(5)
	2.018(6)	1.991(4)	1.983(5)
	2.130(5)	2.132(4)	2.131(5)
	2.169(6)	2.146(3)	2.131(5)

[a] O_t: terminal O atom; Ar: 1,2-dihydroxybenzene ligand.

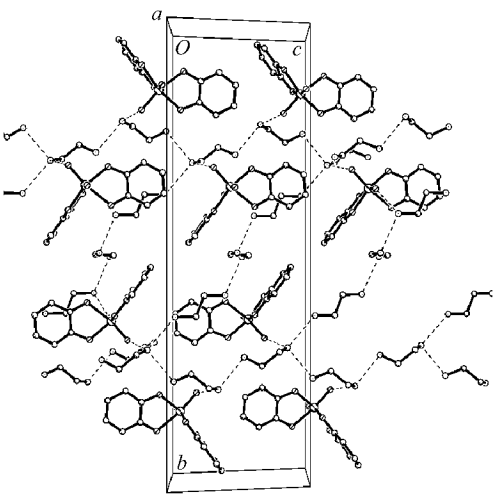

Fig. 2 Packing diagram of complex **1**.

UV-vis *observation*

It is obviously that there are distinct and significant differences in the UV-vis absorption for the three complexes in Fig. 3. In the spectra of $(NH_3CH_2CH_2NH_2)_3[Mo^{(V)}O_2(OC_6H_4O)_2]$ (the dotted line in Fig. 3), the band at 365 ($\varepsilon = 3.4 \times 10^3$) nm is assigned to 1,2-dihydroxybenzomolybdenum(V) charge transfer, and the band at 280 ($\varepsilon = 2.6 \times 10^4$) nm is associated with ligand $n \rightarrow \pi^*$ and

π-π^* transition. Otherwise, there is only one broad signal which covers the range from 280 nm to 365 nm in the UV-vis spectra of $(NH_3CH_2CH_2NH_2)_2[W^{(VI)}O_2(OC_6H_4O)_2]$ (the dashed line in Fig. 3) because of d^0 electronic configuration of W(VI) in the complex. For $(NH_3CH_2CH_2NH_2)_{2.5}[Mo^{(V)}_{0.5}W^{(VI)}_{0.5}O_2(OC_6H_4O)_2]$, a transient UV-vis absorption spectrum is observed between the UV-vis spectra of complexes **1** and **3** (the solid line in Fig. 3), though the absorption at 365 nm produced by 1, 2-dihydroxybenzo-molybdenum charge transfer and 280 nm resulted from $n\rightarrow\pi^*$ and π-π^* transition are still there, but the peaks are broadened largely.

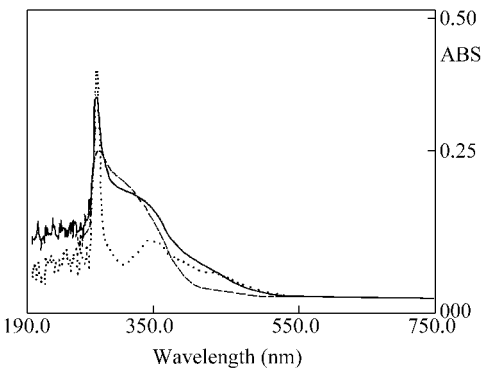

Fig. 3 UV-vis spectra of complex **1** (solid line), complex **2** (dotted line) and complex **3** (dashed line) in H_2O.

EPR *observation*

The EPR spectra of the complexes were recorded as powder at room temperature. $(NH_3CH_2CH_2NH_2)_3[Mo^{(V)}O_2(OC_6H_4O)_2]$ and $(NH_3CH_2CH_2NH_2)_{2.5}[Mo^{(V)}_{0.5}W^{(VI)}_{0.5}O_2(OC_6H_4O)_2]$ are active to EPR while $(NH_3CH_2CH_2NH_2)_2[W^{(VI)}O_2(OC_6H_4O)_2]$ is EPR silent, which is in agreement with the result of the UV-vis spectra of the complexes. Another notable feature is the width of the peaks of the EPR spectra in Fig. 4(a) and Fig. 4(b). The reason that the peaks in Fig. 4(a) are much wider and lower than that in Fig. 4(b) is secular broadening effect which relates directly to the distance between the paramagnetic ions by the ratio of $(3-\cos^2\theta)/r$. The distance between $Mo^{(V)}$ ions in the crystal of complex **2** is only a half of the distance between $Mo^{(V)}$ ions in the crystal of complex **1**, so that the secular broadening effect in $[Mo^{(V)}O_2(OC_6H_4O)_2]^{3-}$ is more than that in $[Mo^{(V)}_{0.5}W^{(VI)}_{0.5}O_2(OC_6H_4O)_2]^{2.5-}$, and the resolution and sensitivity of the signal in Fig. 4(a) is less than those in Fig. 4(b). It is more worthy to pay attention to that the EPR spectra exhibited by complexes **1** and **2** are similar to that of flavoenzyme [Fig. 4(c)].[11] As

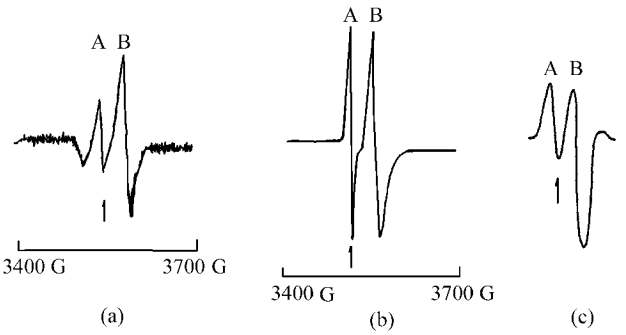

Fig. 4 EPR spectra of complex **1** (b) and complex **2** (a) at 288 K and flavoenzyme (c) at 100 K.

shown in the EPR spectra of flavoenzyme the signal labeled by letter A is assigned to the ligand of FMN in flavoenzyme from milk, the peak labeled B arises from the field of Mo(V). Similarly, in the EPR spectra of complexes **1** and **2**, the A signals are attributed to the 1,2-dihydroxybenzo ligand and the B peaks arise from the field of Mo(V). Unlike NMR, IR and UV spectroscopy and electrochemical studies, EPR parameters of the complex in the Mo(V) state are essentially invariant with respect to the substituent, the predominant effect which affects the EPR spectra is the coordination structure of the complex. The similarity of the EPR spectra of complexes **1** and **2**, and flavoenzyme indicated that the three substances might have the same coordination feature.

References

1 Hille, R. *Chem. Rev.* **1996**, *96*, 2757.
2 Michael, K. J.; Douglas, C. R.; Michael, W. W. A. *Chem. Rev.* **1996**, *96*, 2817.
3 Lim, B. S.; Donahue, J. P.; Holm, R. H. *Inorg. Chem.* **2000**, *39*, 263.
4 Lim, B. S.; Willer, M. W.; Holm, R. H. *J. Am. Chem. Soc.* **2000**, *123*, 8343.
5 Sung, K. M.; Holm, R. H. *J. Am. Chem. Soc.* **2000**, *123*, 1931.
6 Thomson, L. M.; Hall, M. B. *J. Am. Chem. Soc.* **2001**, *123*, 3995.
7 Lim, B. S.; Holm, R. H. *J. Am. Chem. Soc.* **2001**, *123*, 1920.
8 Graham, N. G.; James, H.; Carrie, T.; Roger, C. P.; Rajagopalan, K. V. *J. Am. Chem. Soc.* **1999**, *121*, 1256.
9 Lu, X. M.; Liu, S. C.; Mao, X. A.; Bu, X. H. *J. Mol. Struct.* **2001**, *562*, 89.
10 Lu, X. M.; Liu, S. C.; Jiang, L.; Mao, X. A. *Chin. J. Chem.* **2003**, *21*, 650.
11 Bray, R.; Malmström, B.; Vänngärd, T. *Biochem. J.* **1959**, *73*, 193.

(E0211154 ZHAO, X. J.; LU, Z. S.)